ISBN: 978-3-95450-250-9 ISSN: 2673-5520 doi:10.18429/JACoW-MEDSI2023-TUOAM02

UPDATE OF THE BM18 ESRF BEAMLINE DEVELOPMENT: PRESENTATION OF SELECTED EQUIPMENT AND THEIR COMMISSIONING

F. Cianciosi†, A.-L. Buisson, P. Carceller, P. Tafforeau, P. Van Vaerenbergh, ESRF, Grenoble, France

Abstract

This article highlights specific equipment that have not yet been described in previous publications, notably the in-vacuum cooled fast shutter for high-energy, the wide aluminium window and tailored high-precision slits (400 × 200 mm opening). 2022 and 2023 have seen the installation and commissioning of these new equipment. The ID18 beamline opened for user applications in September 2022 with limited capabilities and has been increasing its possibilities since then. It is expected to be fully equipped by the end of 2024.

INTRODUCTION AND BEAMLINE PERFORMANCES

The ESRF-EBS beamline BM18 has been tailored for hierarchical propagation phase-contrast tomography. The 220 m long beamline benefits from a high-coherence at high-energy beam from a 1.56 T triple short wiggler of the new 4th generation storage ring. The beamline combines a resolution range from 120 µm down to 0.65 µm with the possibility to scan samples up to 2.5 m high and 1.2 m in diameter. With a beam width up to 35 cm and energies ranging from 40 to 280 keV (polychromatic), the main applications are material sciences, cultural heritage, geology, biomedical imaging and industrial applications.

Due to the delays in the development and installation of the large sample stage previously described in [1], the beamline started user operation in September 2022 using a new version of a smaller sample stage initially developed by *LAB Motion Systems* in 2012 for palaeontology on the ID19 (2 stages) and ID17 (1 stage) beamlines and of which two more copies were installed later on BM05. The maximum dimensions of samples are therefore limited to 30cm in diameter, 30 kg in weight, and 50 cm vertically. Once the large sample stage is operational, the maximum dimensions will be 1.2 m diameter, 300 kg and 2.5 m vertically.

IN-VACUUM COOLED FAST SHUTTER

During the commissioning and the initial operation of the BM18 beamline, the quick obturation of the photon beam was made using the photon absorber placed at the end of the Optical Hutch. However, this instrument is not optimal for this purpose, because it is relatively slow (about 1s/cycle), it has a relatively short life (about 100k cycles) and it is part of the safety equipment of the beamline, therefore its use should be reserved to this function only.

For an impinging power of 300 W, and a beam size of 100 × 5 mm, it was decided to develop a specific beam shutter with the aim of shutting off the beam quickly (maximum opening/closing time: 0.1 s), the possibility of continuous operation (i.e. frequency: 1 Hz) and for a long-life (several millions of cycles).

The shutter itself is constituted by a tungsten blade, which rotates by 30° to either intercept the beam or let it pass. It is actioned by a cooled stepper motor. All the components are in vacuum. The blade is isolated from the shaft by a PEEK spacer. When the blade is in the upper position, it remains in contact with a water-cooled copper block which cools the tungsten blade. This block is mounted on springs to ensure good contact pressure with the blade and a perfect alignment between the contact surfaces. Figure 1 shows the blade in the open position (the blade in closed position is superimposed in transparency).

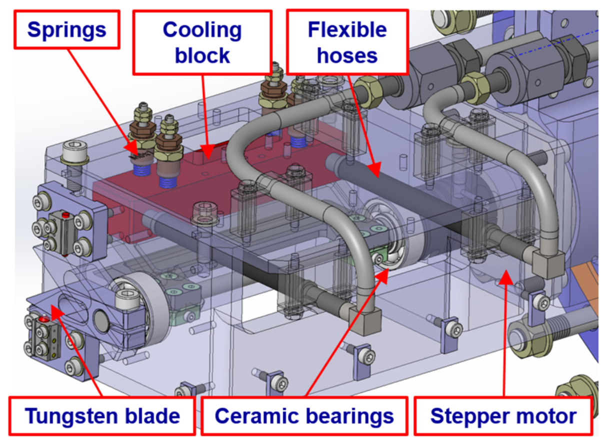

Figure 1: Design of the in-vacuum cooled fast shutter.

Calculated pressure contact between the blade and the cooling block is 0.85 bar. FEA calculations (Fig. 2) demonstrate that, for a thermal contact exchange coefficient of 800W/m²K [2], the blade would not exceed 214 degrees more than that of the cooling water temperature (20 ºC).

The control of the motor is done with an IcePAP controller [3] and the software is under development.

The foreseen closing movement will be done in two phases: a quick rotation to intercept the beam in the required time, followed by a slower movement to ensure contact with the cooling block.

The manufacturing drawings have been completed and the parts have been ordered. The assembly will be done at ESRF and the first test is scheduled before the end of 2023.

† cianciosi@esrf.fr

ISBN: 978-3-95450-250-9 ISSN: 2673-5520 doi:10.18429/JACoW-MEDSI2023-TUOAM02

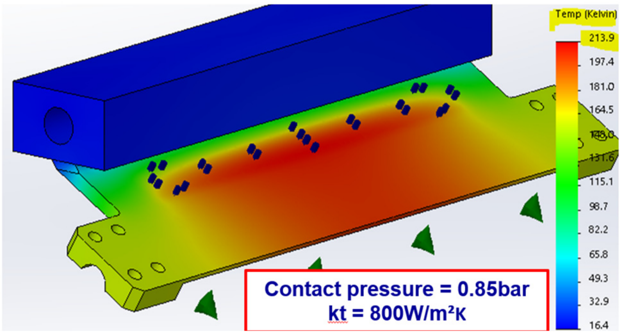

Figure 2: Temperature rise of the tungsten blade relative to the water temperature.

WIDE ALUMINIUM WINDOW

At the entrance of the Experimental Hutch (EH), the beam will go from vacuum to air. For that, a large vacuum-tight window is required, to allow a wide beam (i.e. 400 (h) × 200 (v) mm) to pass. The selection of the material, and the design of this component, was demanding. The window has to let the full wide beam pass (without reducing it), it has to sustain a 1bar pressure difference while heated by the beam and it has to be as transparent as possible to the radiation (up to 50 W would be absorbed by the window if using the full beam size without any filter in the optics hutch). In addition, the selected material has to be easy to polish close to an optical grade (i.e. Ra < 0.1) [1].

The selected design was a relatively simple membrane-type window made of aluminium (very low alloyed, "half-hard" state). The material has been sourced from *Goodfellow* (reference: AL00-FL-000300; purity of 99%).

The metallic membrane is clamped to a stainless-steel flange. The vacuum tightness is obtained by a Viton gasket (Fig. 3). Calculations show that, under pressure, a 1mm thick window would exceed the elastic limit with 2 % strain induced (Fig. 4).

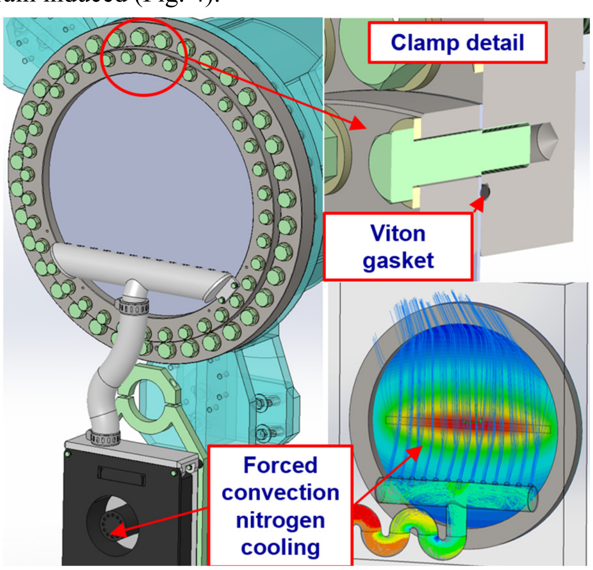

Figure 3: Design and thermal simulation of the membrane.

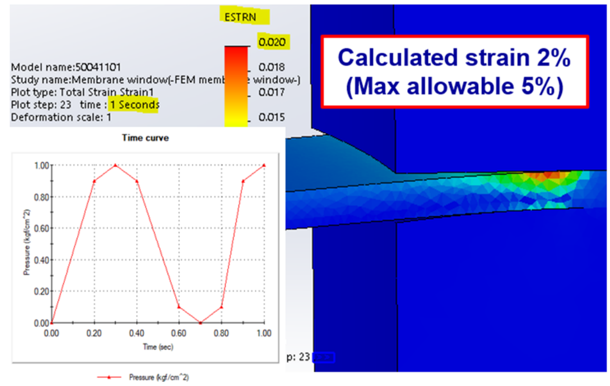

Figure 4: Strain calculation of the membrane showing a deformation of 2 % (5% is the failure deformation obtained during the collapsing tests).

It has to be pointed out that the relation between pressure and strain is not linear due to the geometrical shape. By increasing the pressure, the metallic membrane develops a dome shape which is more efficient in resisting the load.

ESRF has purchased several sheets of this material with thicknesses of 1, 1.2 and 2 mm (coming from the same production batch). This has permitted real-scale testing as well as making the final production of the window with exactly the same material. The mechanical characteristics, measured during the testing of this material is shown in Table 1.

Table 1: Mechanical Characteristics of the AL00-FL-000300 at 2 Temperatures

	20°C	100°C
Yield stress	115 MPa	97.5 MPa
Rupture stress	123 MPa	100 MPa
Max strain	5.2%	ND

The real-scale tests, performed by increasing pressure with water on the future air-side, has been repeated on the 3 available thicknesses. Tests have demonstrated a safety factor, regarding the load, always bigger than 3 even when using a 1mm thick membrane (Fig. 5). Therefore, the 1mm thickness has been selected for the production of the installed window.

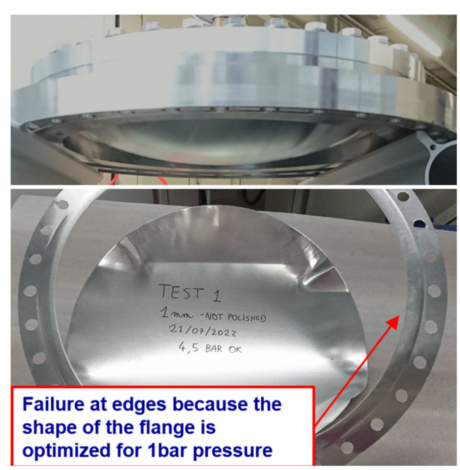

Figure 5: Aluminium window during water pressure test.

ISBN: 978-3-95450-250-9 ISSN: 2673-5520 doi:10.18429/JACoW-MEDSI2023-TUOAM02

The polishing was done by the BM18 scientist, who acquired good knowledge in this field thanks to his experience with fine polishing of filters and sample preparation.

QUINARY SLITS

Large aperture slits are settled downstream of the large window, inside a PETG chamber flushed by nitrogen (Fig. 6). They are composed of 4 tungsten blades of dimensions 400 (h) × 200 (v) mm height and 20 mm thick. They are equipped with an inner cooling loop and designed to accommodate the full beam (i.e. 400 × 20 mm in white beam mode and up to 350 × 200 mm with the current development to have an enlarged monochromatic beam). They are able to sustain the full impinging power of 300 W. The minimum vertical gap achievable is 20 µm with a measured parallelism error of 5 µrad. Their Minimum Incremental Motion (MIM) is 1 µm, their repeatability is in the order of 1.5 µm as well as their stability over a week.

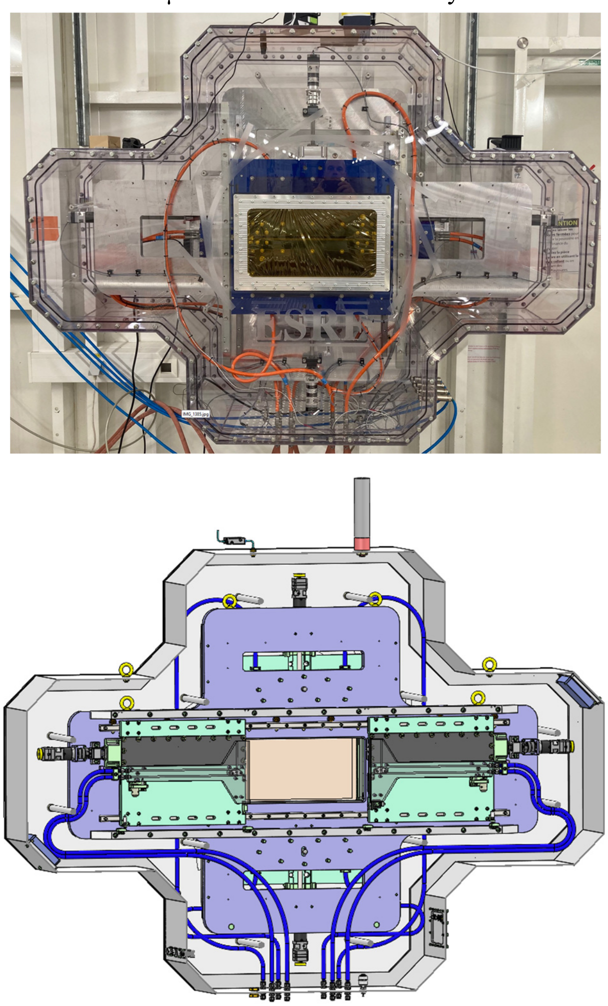

Figure 6: Picture and layout of the quinary slits inside the nitrogen box. A 25 µm Kapton window has been installed for 7 months now without failure.

DETECTOR GIRDER

The detector girder is the structure supporting the detectors and related equipment, for a total payload of about 3T. It has to move over 30 m along the hutch, and is compounded by a steel structure (2T) supporting a granite slab (3T). An additional trolley is used to carry controllers for the motorised stages and computers for the detectors (Fig. 7) [1].

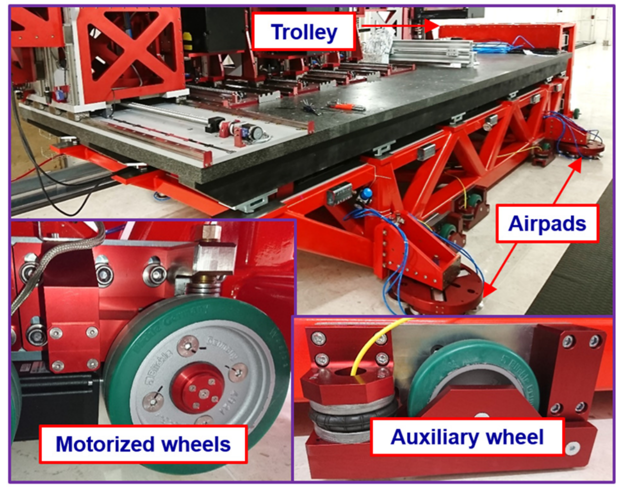

Figure 7: Detector girder on airpads. Details of motorized wheels and auxiliary wheels.

In the original design, the girder was placed on 4 groups of 6 precision airpads from *Positechnics* D160 mm, hovering above the marble floor of EH (140 m^2). Unfortunately, and despite the efforts of the supplier, this floor presented some local defects that made the motion of the airpads very difficult. The air gap for this type of pad is a function of the applied load and the feed pressure. For our application, this value is in the range of a few tenths of microns. Despite many polishing campaigns, the girder still did not move smoothly.

The solution that we have developed is based on wheels. It includes 7 auxiliary wheels (located over the periphery of the frame) and 4 main wheels (located at the 4 corners). The aim of the auxiliary wheels (already installed) is only to relieve the load. They are actuated pneumatically and they have no stroke limit. The 4 additional main wheels will replace the airpads. They will be actuated pneumatically too but their stroke is limited mechanically to lift the girder to the desired necessary value (i.e. around 1mm) as shown in Figs. 8 and 9. Four motorized wheels, instead of one, will be needed to overcome the greater friction of the wheels as compared to the former airpads. During the image acquisition, the air-pressure in the bellows will be removed in order that the girder may rest on aluminium pads for maximum stability and position repeatability.

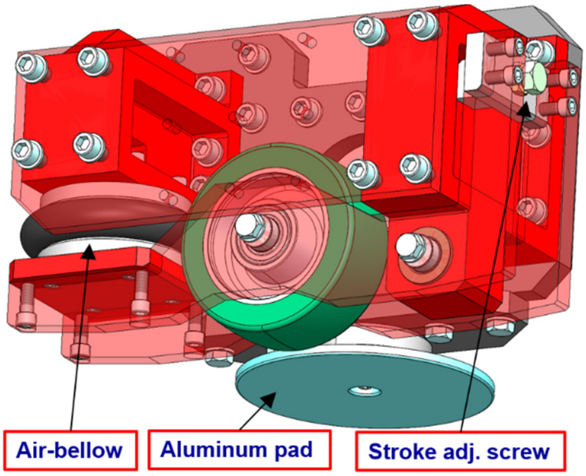

Figure 8: Main wheels to replace of the airpads.

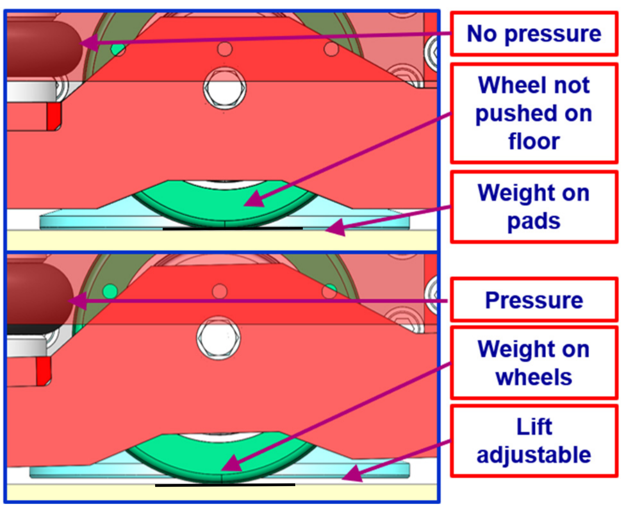

Figure 9: Main wheels in retracted position (top figure) and in contact with the floor (bottom figure).

DETECTOR STAGES

The detector girder is equipped with 9 combined stages (Fig. 10) with 600 mm stroke on the vertical and horizontal axes.

The beamline is currently equipped with 8 different detectors, covering pixel sizes from 0.65 µm to 120 µm. Additional optics are still in the development phase and will be implemented in 2024 and 2025. Each stage can host detectors from 50 kg to 200 kg. The maximal detector size is 700 × 900 × 500 mm. MIM of this equipment is 1 µm as well as the repeatability. Over 6 consecutive days of experiments, the stability was still within a single pixel size of the detector used for this experiment (i.e. 6 µm).

Figure 10: Two of the detector stages (in red), hosting detectors (in black).

CONCLUSIONS

After more than a year of commissioning and experiments, BM18 has largely fulfilled its goals. The main unfulfilled goal is evidently the use of the large sample stage for user experiments. This is expected to become a reality by mid-2024 based on the present state of the installation. The sample stage will be unique in the world in terms of sample size that can be accommodated for high-resolution imaging.

BM18 is already a highly subscribed beamline, both for academic research and for industrial applications. Most of the installed equipment are prototypes, based on cutting-edge technology and thus still require time and effort for final characterisation and optimization.

ACKNOWLEDGEMENTS

The BM18 project team wish to thank the *LAB Motion Systems* staff for their determination and diverse expertise. The BM18 project is partially funded by the German Federal Ministry of Education and Research (BMBF), in collaboration with the Fraunhofer Gesellschaft, the Julius-Maximilians-Universität Würzburg, and the Universität Passau.

REFERENCES

[1] F. Cianciosi *et al.*, “BM18, the new ESRF-EBS beamline for hierarchical phase-contrast tomography”, in *Proc. MEDSI'20,* Chicago, USA, Jul. 2021, pp. 1-5. doi:10.18429/JACoW-MEDSI2020-MOIO02

[2] B. Fell and K. Fayz, “Thermal contact resistance experimental investigation on the cooling of PHOENZ-UV mirror M1”, CLRC Daresbury Laboratory, UK, Rep. 107.51520, May 2020.

[3] N. Janvier *et al.*, “IcePAP: an advanced motor controller for scientific applications in large user facilities”, in *Proc. ICALEPS'13,* San Francisco, CA, USA, Oct. 2013, paper TUPPC081, pp. 766-769.